# Design and Characterization of a Haptic Paddle for Dynamics Education

Chad G. Rose *  James A. French †  Marcia K. O'Malley‡

Rice University

**Abstract**

A single axis force feedback device known as a haptic paddle has been implemented as a teaching tool at several universities with different designs and emphases. Presented here is a low-cost haptic paddle design that increases the ease with which students can assemble and perform virtual environment experiments over that of previously presented designs, without decreasing the haptic performance below acceptable levels. We present a frequency domain system identification and Z-Width performance characterization of the new design alongside a comparison to the previous Rice University haptic paddle design. Lastly, we discuss the benefits of new real-time hardware, an easy-to-use Field-Programmable Gate Array (FPGA), implemented with the haptic paddle.

**Index Terms:** H.5.2 [User Interfaces]: Haptic I/O—Training, help and documentation; K.3.1 [Computer Uses in Education]: Collaborative learning—Computer-assisted instruction

## 1 Introduction

A key challenge in engineering courses is offering students the chance to interact with physical systems in the real world to complement the theoretical lecture component. Part of this challenge lies in developing a low-cost, robust system that can deliver the performance necessary to display system dynamics that can be understood by students. On the other hand, it is crucial that this device has intrinsic characteristics that make it applicable to a wide range of educational pursuits. Haptic paddles, an example of which is seen in Fig. 1, are ideal platforms for conveying to students the underlying principles that are taught in undergraduate system dynamics classes. Possessing nonlinear dynamics, integrated (multi-domain) system dynamics, adaptability to basic control theory, graphic programming, and real-time hardware implementation, this simple one degree of freedom (DOF) device forms a basis for the introduction and implementation of many topics covered in the undergraduate mechanical engineering curriculum.

Since the deployment of the haptic paddle in 1997 [16], several universities have iterated on the design (see Table 1 for a summary). All have a few basic components, as seen in Fig. 2. The end effector, where the students interact with the paddle, and sector pulley are generally one piece. This is connected to a pivot point on the base, and a DC motor via the motor spool, forming the paddle's transmission. The sensing in the paddles typically occurs at the pivot point, either through Hall Effect sensors or similar low-cost magnetic position sensors.

The different designs at each university serve similar purposes, and the myriad of variations on the basic design reflect the emphases placed on each device at its respective institution. In the past 15 years of haptic paddle implementation, there have been a few studies concerning the effectiveness of the haptic paddle as a pedagogic tool, ranging from qualitative and anecdotal to organized, quantitative measures [3, 7, 9, 17]. The spectrum of haptic paddle designs contains a wide variety of sensing, actuation, and computation methods that are reflected in the total cost and performance level achieved. In particular, the devices used at the University of Michigan, the iTouch and the Box [8], seem to represent the two end goals of these devices. The iTouch uses student built voice coil actuators, which have lower performance than some of the commercial actuators used. However, the cited pedagogic benefit outweighs the loss in performance. The Box, on the other hand, is a self-contained unit aimed at creating higher quality haptic displays, and its design and cost reflect that. In order to work towards the same goals set out by the University of Michigan devices (namely, more undergraduate education focus, or higher quality testbed for advanced education or research), some design changes have been made to the original proposed design by Richard et. al, [16]. Specifically, some paddles have switched to a new design for the user interface pendulum, where the sector pulley and end effector are separated by the pivot point of the device, moving the motor down to the base of the paddle [1, 2, 3, 7, 9]. Secondly, some have added optical encoders, either to replace or be used in conjunction with magnetic position sensors, in order to achieve more accurate sensing [7, 8, 9, 16]. Nearly every paddle design utilizes different implementation hardware, from purpose built, custom electrical circuits and C++ code to off-the-shelf components and industry-grade software tools. Finally, one of the more recent developments is the adoption of a friction drive [2, 9] to replace the capstan. The results of this design change will be investigated further in Sections 3 and 4.

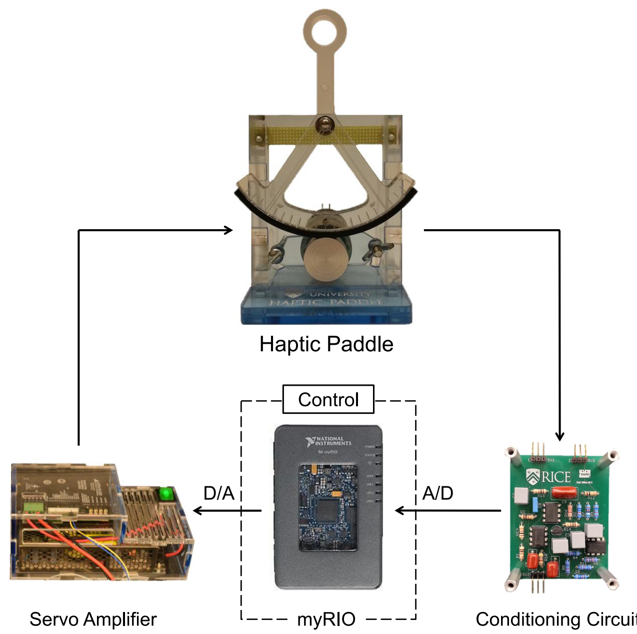


Figure 1: Rice Friction Drive Paddle, servo amplifier, NI myRIO, and analog signal conditioning circuit

*e-mail: cgr2@rice.edu
†e-mail: jaf12@rice.edu
‡e-mail: omalleym@rice.edu

IEEE Haptics Symposium 2014
23-26 February, Houston, Tx, USA
978-1-4799-3131-6/14/$31.00 ©2014 IEEE

| University | Year | Course | Actuation | Transmission | Reported Cost |
|---|---|---|---|---|---|
| Stanford [16] | 1997 | UG Linear Systems | DC motor | Capstan drive | $30 + D/A I/O |
| Univ. of Michigan iTouch [8] | 2003 | UG Linear Systems | Custom voice coil | Direct drive | $20 |
| Univ. of Michigan The Box [8] | 2003 | Senior-level Embedded Control/Research Application | DC motor | Gear/cable-chain | $600 |
| Rice Univ. Capstan Drive [3, 4] | 2006 | UG Linear Systems | DC motor | Capstan drive | $50 + D/A I/O |
| Johns Hopkins [17] | 2007 | UG Linear Systems, Adv. Interdisc. Course. | DC motor | Capstan drive | $30 + D/A I/O |
| Vanderbilt [9] | 2009 | UG Intro/Linear Systems, Gr. Haptic and Virtual Env. | DC motor | Friction drive | $200 |
| Univ. of Utah [1] | 2009 | UG Robotics for ME/CS | DC motor | Capstan drive | $650 |
| ETHZ [7] | 2012 | UG Dynamics and pHRI | DC motor | Capstan drive | $350 + D/A I/O |
| Rice Univ. Friction Drive | 2012 | UG Linear Systems | DC motor | Friction drive | $50 + D/A I/O |
| Stanford [2] | 2013 | UG Intro to Engineering | DC motor | Capstan Drive | $50 |

Table 1: Haptic paddle design overview

This paper presents a new design of the haptic paddle, along with new, low cost, real-time hardware designed for educational use (Section 2). Furthermore, the device characterization of the new Rice Friction Drive Haptic Paddle and our previously used Capstan Drive Haptic Paddle (Section 3) is a valuable addition to the literature on the haptic paddle and similar devices. Lastly, in order to further investigate the performance of the new design, this paper presents the Z-Width characterization of both the new and previous Rice haptic paddle designs (Section 4).

## 2 Design Overview

While conducting laboratory experiments with the original Rice Haptic paddle, the need to rewind the capstan transmission as a result of system instability or prolonged use resulting in cable stretch was identified as an all too frequent and time costly exercise for both students and laboratory teaching assistants. To solve this problem, and maximize the efficiency of lab time, a new, more robust transmission, a friction drive, was designed. The goal of the new design was to eliminate these problems while maintaining a level of hardware performance suitable for a pedagogic environment. Hardware and software limitations and stops could be placed on the haptic paddle to prevent instability. However, we believe that allowing students to experiment with and safely experience stable, neutrally stable, and unstable configurations of the haptic paddle has strong pedagogic benefit.

The Rice Friction Drive Haptic Paddle design consists of an acrylic handle that rotates around a central pivot point. A grip point is located above the pivot point, and a curved surface of constant radius is located below the pivot point. The system uses an Allegro Microsystems A1322 ratiometric linear Hall Effect sensor for position sensing, a custom-built analog signal conditioning circuit for amplifying and scaling the analog position signal, an Advanced Motion Controls 12A8M PWM servo amplifier for driving a Pittman 9434 15.1V DC motor, and a friction drive transmission. The friction drive consists of a 1.25” diameter aluminum cylinder mounted on the output shaft of the DC motor and neoprene tape attached to the curved surface of the paddle. The motor height, and hence the normal force on the friction drive, are made adjustable by two accessible wing nuts on opposite sides of the motor, free to slide in a slot. This height is adjusted by the students in the course of the laboratory experiments, in order to determine the effects of normal force between the friction drive and the paddle on the rendered virtual environment or teleoperation. The primary motivation for using a friction drive is its robust design that is both easy to install and adjust in a learning environment.

The previous iteration of the Rice University haptic paddle, the Capstan Drive Paddle, employed a capstan cable transmission for low backlash and high efficiency [3, 4]. Although this design allowed for a high quality haptic interface, the cable was susceptible to becoming unwound and disengaged when the students experimented with unstable dynamic systems. This often necessitated laboratory teaching assistant intervention and lab time not spent engaged with a haptic device, whereas the friction drive is more robust, giving the students more hands-on time to experiment. During unstable configurations, the friction drive is able to rotate outside its range of motion, effectively disengaging the motor spindle from the neoprene tape.

Another notable difference between the two designs is the size of the motor spools. In order to create a sufficient contact patch for the friction drive transmission, the motor spool (i.e. the aluminum cylinder) needed a larger diameter than that of the motor spool in the cable transmission. The use of a larger motor spool reduced the gear ratio from about 17:1 with the cable drive paddle to 4.8:1 with the friction drive paddle. This reduces the apparent inertia felt by the user, as the motor spins less for a given input at the paddle handle. The results of this gear ratio change will be further examined in Section 3. Quantitative device comparisons in the following sections will show the effects of the new transmission design and reduction in gear ratio on the quality of rendered haptic environments, and lend support to the use of the new Rice Friction Drive Haptic Paddle design in pedagogic laboratory experiments.

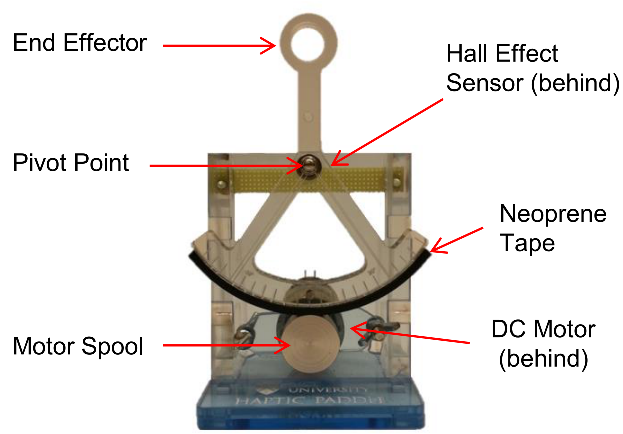


Figure 2: Overview of the Rice Friction Drive Haptic Paddle

### 2.1 Data Acquisition and Control

The raw position and velocity signals from the Hall effect sensor are filtered using a second order, active filter. The Conditioning Circuit then has components for offset removal, differentiation, and amplification. These processed signals are then sent to hardware and software from National Instruments (NI) for real time control. A proportional-derivative (PD) controller acting on paddle position was implemented within LabVIEW. On the front panel, the students are able to view and change important system parameters, such as the control loop rate, virtual wall stiffness, and virtual wall damping. The paddle position, angular velocity, and control signal are plotted versus time so that the students can witness the functioning of the controller. To maximize the performance of the system, the NI myRIO was chosen as the data acquisition and control hardware. This device provides analog input and output channels that have an effective operating range of $\pm 10$ V with 12 bit ADC/DAC resolution. These are the only channels required to read the position signal from the signal conditioning circuit and send the control signal to the servo amplifier. A notable feature of this device is its high-performance FPGA, which enables fast closed-loop control. For rendering haptic environments such as virtual walls, a loop rate of 100-500 Hz is acceptable ([7] used 100Hz and 500Hz for Z-Width tests). This magnitude of loop rates was achievable with the NI myDAQ, a device that is very good for data acquisition but is not designed for high-speed, closed-loop control. A faster loop rate is desired because it allows for rendering of greater virtual wall stiffness and damping [7, 14].

Since the control program developed in LabVIEW can be downloaded to the NI myRIO, eliminating latency issues with the USB port, much higher loop rates are attainable than with a controller running solely on a desktop computer. This allows for the implementation of more performance-intensive virtual environments, such as teleoperation. In previous years, teleoperation, which is used as the culmination of the lab experience in the system dynamics course, was performed using a NI PXI. The NI PXI is a modular instrumentation PC-based standard for measurement and automation systems, designed for industry applications. The performance of this device was more than adequate for implementing a teleoperation control scheme, which necessitates control loop rates on the order of 1,000 Hz [12]. However, the device was less accessible to the students and functioned more as a black box that the teaching assistants configured. The NI myRIO was attractive for a lab setting due to it its ease of use, plug-and-play features and level of performance. During an early access program with NI, a loop rate of 2,000 Hz was achieved in teleoperation tests without the need for re-programming the low-level FPGA. Much faster loop rates are surely attainable if the control algorithm is programmed into the FPGA. This, although anecdotal in nature, is included here to support the claims that hardware such as the NI myRIO is both easy for students to use, and also has sufficient performance for the time-critical control of virtual environments and teleoperation. In conducting the experiments to evaluate the performance of the cable drive- and friction drive paddles, the myRIO was used as the controller hardware to relate to the actual teaching lab environment.

## 3 SYSTEM PARAMETER IDENTIFICATION

In order to evaluate the haptic paddle as a mechatronic device, its system characteristics need to be known. To date, the only system characterization of a haptic paddle that has been performed has been via time domain techniques. For this reason, this paper presents a frequency domain characterization of two haptic paddles, the newly adopted Rice Friction Drive Paddle, and the Rice Capstan Drive Paddle.

### 3.1 Experimental Protocol

A key assumption during this characterization was that the dynamics of a haptic paddle could be sufficiently modeled as a first order system in velocity, as shown below,

$$m\dot{v} + bv = \tau \qquad (1)$$

where $\tau$ is the torque input of the motor. This model was selected for two reasons, namely that it captures most of the system response, and provides an experimental platform to explore first order system behavior that the students have learned in the lecture portion of the course. The goal of this experiment was to determine the values of the $m$ and $b$ terms in this model. To perform frequency domain analysis of the haptic paddle, a Schroeder phased input signal was used in order to generate the frequency response of the haptic paddle between 1 and 20 Hz [15]. The Schroeder phased input signal is desirable for frequency analysis because its power spectrum is flat in the region of interest, better capturing the dynamics of the system. The region of interest was chosen since human users cannot interact with haptic devices in a controlled manner above 10 Hz, but the signals generated by PD controllers can generate signals of higher frequencies [10].

### 3.2 Frequency Domain System Identification

The coherence plots for these Schroeder waveforms for the Friction Drive Paddle and the Capstan Drive Paddle are shown below in Fig. 3.

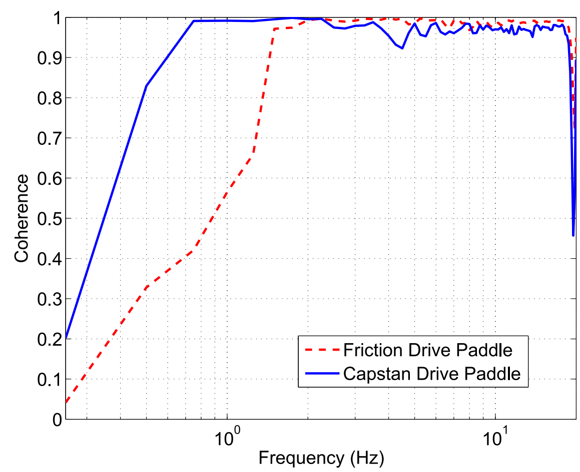


Figure 3: Coherence between Schroeder multiwave input and velocity output for Rice Friction Drive Paddle and Rice Capstan Drive Paddle

The high coherence value for both of these systems should lend credence to the accuracy of the experimental transfer function representing the dynamics of the Rice Friction Drive Paddle and the Rice Capstan Drive Paddle, shown in Fig. 4 and Fig. 5, respectively.

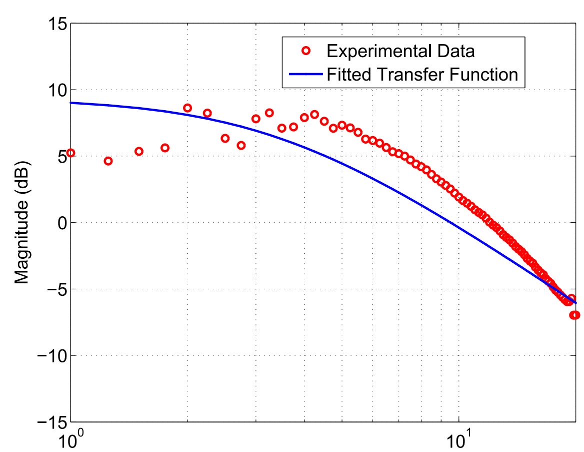


Figure 4: Bode plot of experimental data and fitted transfer function for Friction Drive Paddle

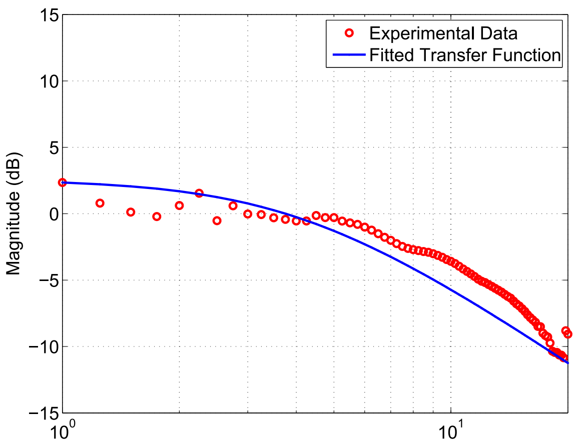


Figure 5: Bode plot of experimental data and fitted transfer function for Capstan Drive Paddle

Table 2: Experimentally determined $m$ and $b$ values

| | Friction Drive Paddle | Capstan Drive Paddle |
|---|---|---|
| $m\ [kg \cdot m^2]$ | 0.01573 | 0.0284 |
| $b\ [\frac{N \cdot m \cdot s}{rad}]$ | 0.3405 | 0.7417 |

These Bode plots of the experimental and fitted data (the quotient of the cross power spectral density and the power spectral density $\frac{P_{yx}(f)}{P_{xx}(f)}$, where $x, y$ are input and output, respectively) exhibit a few common characteristics. First, the close match between the experimental data and the fitted first order transfer function support the claim that the haptic paddle can be sufficiently modeled by the proposed first order differential equation for the purposes of this undergraduate course. Secondly, the spread of the data around low frequencies is indicative of the relative difficulty of using low frequency signals for system identification, especially due to the workspace limitations of both paddles. When comparing the fit of the estimated transfer functions of the Friction Drive Paddle and the Capstan Drive Paddle, one should note that the Capstan Drive Paddle's data seems to fit the model better. This could be, in part, due to some nonlinearities introduced by the friction drive itself, such as the non-uniform nature of the neoprene tape or slight misalignments between the paddle and the motor spool.

Of note when examining the system parameters in Table 2 is that they are all likely overestimated. This is plausible because the first-order linear model, although sufficient for capturing the majority of the system's dynamics, does not take into account the inherent non-linear trigonometric relationships in these rotational systems, nor the effects of other non-linearities such as the misalignment of the paddle and friction drive, the friction inherent to the neoprene tape, or the slight flex of the press-fit acrylic haptic paddle supports. Nonetheless, as a tool for comparison, these slightly overestimated values serve as a valid metric, since any overestimation affects both paddles. When comparing the two paddles, it is seen in the data (and felt while using the unpowered device) that the capstan drive paddle has greater reflected damping and inertia due to the higher gear ratio. If steps are not taken to cancel these during teleoperation, they could have a significant detrimental effect on the teleoperation experience.

## 4 Virtual Environment Performance Characterization

One of the most common performance metrics for haptic devices is the Z-Width. It is defined as the dynamic range of achievable impedances that can be passively rendered [6]. This creates not only a standard to compare to other devices, but also a useful tool in determining the stable functioning limits of a system.

### 4.1 Experimental Protocol

The Z-Width experiments were carried out in a manner similar to that proposed in [6], in that passive and non-passive behavior were characterized while the device was being used in its intended manner. In this case, the device was held with a thumb and two finger grip on the top of the haptic paddle pendulum, approximately 2.5 inches away from the pivot point, as shown in Fig. 6. This method was chosen over automated protocols adopted by some [5, 13] in order to present in the literature the performance that a student could expect to see in the lab, and not to quantitatively compare different control structures.

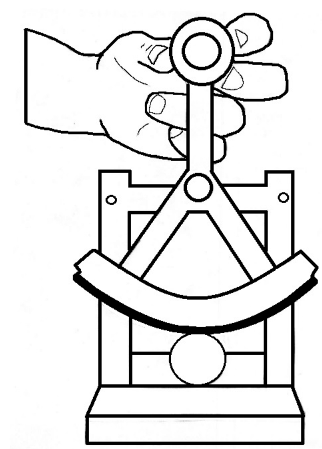

Figure 6: Grip chosen for Z-Width experiments

### 4.2 Z-Width Characterization

In order to determine the shape of the device's Z-Width, an attempt was first made to estimate the maximum virtual damping renderable by the device. Then, with this information, the Z-Width plot was evenly divided, and at each damping step, the maximum virtual wall stiffness renderable was explored. System behavior was classified as nonpassive if there were growing or constant oscillations in the end effector's position, as shown in Fig. 7.

The Z-Width performance of the two paddles is shown in Fig. 8. These rotational units were chosen as the definitive units because the efficiency of the transmissions (capstan and friction drive) was not known, and therefore there exists no guarantee of converting these units into the traditional translational units (N/m, Ns/m) that will accurately reflect the paddles' performance. A determination of the efficiencies of these transmissions would be a good future work for analyzing the performance of these two designs. However, if unity efficiency were assumed ($\tau_{in} V_{in} = \eta \tau_{out} V_{out}, \eta = 1$), the Z-Width could be plotted as seen in Fig. 9.

At first glance, the virtual stiffnesses achieved with low virtual damping by the two paddle designs seen in Fig. 8 and Fig. 9 seem high, especially when compared to industry standard devices. However, these paddles have high physical damping, which has a stabilizing effect on virtual environments with low virtual damping. While the Friction Drive Paddle exhibits a lower Z-Width than the Capstan Drive Paddle, the haptic interface still possesses high

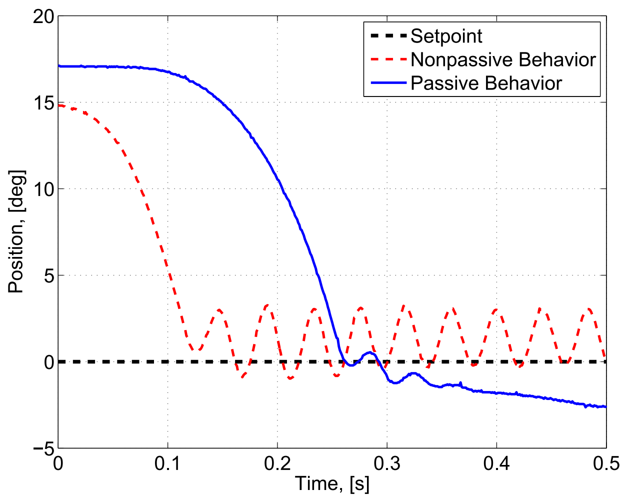


Figure 7: Passive and nonpassive behavior during Z-Width experiments

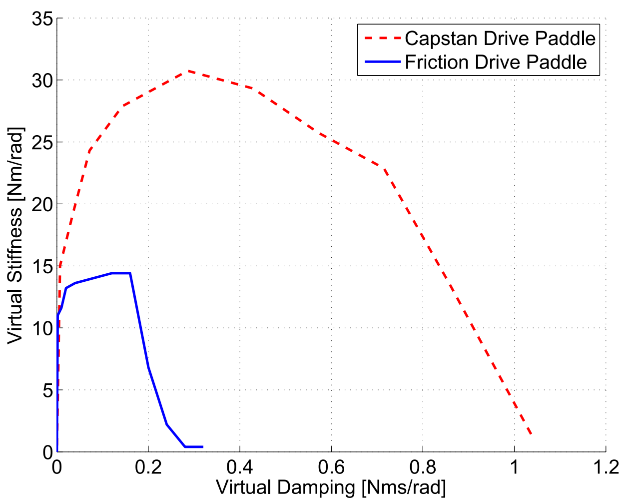


Figure 8: Z-Width plot in rotational units

enough quality to be of instructional value. While higher virtual stiffness and damping values are more desirable for rendering virtual environments, systems with low force feedback levels (on the order of a few Newtons) can still relay significant, discernible haptic information [11].

One noteworthy observation made while performing the Z-Width testing on the Rice Friction Drive Paddle was that the friction drive would slip for very large stiffness values, which tended to flatten out the Z-Width plot, as compared to the smoother plot of the Rice Capstan Drive Paddle's Z-Width. Previously, a Z-Width characterization of a haptic paddle has been presented [7], which was used as a comparison to the Rice University haptic paddles. Of note is that all three paddles possess similar performance values, which serves to validate both tests. The differences between the plots were likely caused by 1) the difference in transmission ratios between the capstan and friction drive paddles and 2) slightly higher performance achieved in the paddles presented here due to the higher control rates (1000 Hz vs 500 Hz) with the myRIO.

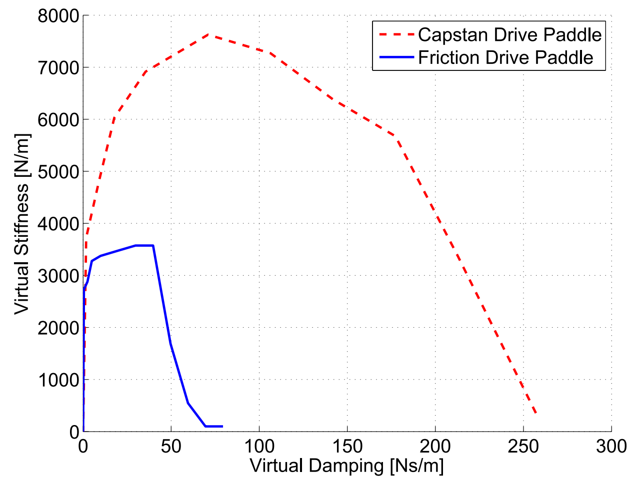


Figure 9: Z-Width plot in linear units, assuming unity transmission efficiency

## 5 Results and Discussion

In this paper, we have presented the design and characterization of the new Rice University Friction Drive Paddle along with the previous design. Key features of the new paddle design are its robust transmission and the real-time control implementation using National Instruments' myRIO hardware. Of note is that the Rice Capstan Drive Paddle exhibits greater Z-Width characteristics, but has larger apparent mass and damping terms. Both of these characteristics are due in large part to the greater transmission ratio of the capstan drive. This amplifies both the motor torque, motor inertia, and motor damping. However, these results support the use of haptic paddles such as the Rice Capstan Drive Paddle in advanced classes or research settings, where higher performance is more desirable. Furthermore, with the performance and I/O functionalities of the myRIO, this would be a suitable testbed for basic research into virtual environments and teleoperation. With the Rice Capstan Drive Paddle, however, improved performance comes at the cost of increased susceptibility to damage based upon student error. Despite the decrease in performance, the Rice Friction Drive paddle is more desirable for undergraduate teaching lab environments, where hands-on time with the device and robustness triumph over performance. Giving students more time to experiment with stable and unstable configurations without degrading performance beyond acceptable levels supports the Rice Friction Drive Paddle as an improved tool for providing students with real-world systems experience.

## 6 Conclusion

The haptic paddle has been shown to be a valuable teaching and laboratory tool for undergraduate and advanced system dynamics, mechatronics, embedded controls courses. Future work on these devices will include more time domain characterization in order to validate the methods used [3, 4, 16] in the curriculum, increasing student involvement in real-time code development, characterization of teleoperation between both paddle designs, further characterization of other haptic paddle designs, and quantitative studies of student learning outcomes.

## Acknowledgements

The authors wish to thank Dr. Vinay Chawda for his gracious help during experimenting and drafting, National Instruments, for providing early access to the myRIO, and Folasade Oba for her work on the design and construction of the Rice Friction Drive Paddle. This work was supported in part by NSF grant CNS-1135916.

## References


[1] Eduhaptics: Haptic paddle designs. http://eduhaptics.org/index.php/HapticDevices/HapticPaddles.

[2] Hapkit: Open hardware haptic device. http://hapkit.stanford.edu/, 2013.

[3] K. Bowen and M. O'Malley. Haptic interfaces for a labview-based system dynamics course. ASEE Annual Conference and Exposition, 2006.

[4] K. Bowen and M. K. O'Malley. Adaptation of haptic interfaces for a labview-based system dynamics course. In *Haptic Interfaces for Virtual Environment and Teleoperator Systems, 2006 14th Symposium on*, pages 147–152. IEEE, 2006.

[5] V. Chawda, O. Celik, and M. K. O'Malley. Application of levant's differentiator for velocity estimation and increased z-width in haptic interfaces. In *World Haptics Conference (WHC), 2011 IEEE*, pages 403–408. IEEE, 2011.

[6] J. E. Colgate and J. M. Brown. Factors affecting the z-width of a haptic display. In *Robotics and Automation, 1994. Proceedings., 1994 IEEE International Conference on*, pages 3205–3210. IEEE, 1994.

[7] R. Gassert, J.-C. Metzger, K. Leuenberger, W. L. Popp, M. R. Tucker, B. Vigaru, R. Zimmermann, and O. Lambercy. Physical student–robot interaction with the ethz haptic paddle. 2013.

[8] R. B. Gillespie, M. Hoffinan, and J. Freudenberg. Haptic interface for hands-on instruction in system dynamics and embedded control. In *Haptic Interfaces for Virtual Environment and Teleoperator Systems, 2003. HAPTICS 2003. Proceedings. 11th Symposium on*, pages 410–415. IEEE, 2003.

[9] J. L. Gorlewicz and R. J. Webster III. A formal assessment of the haptic paddle laboratories in teaching system dynamics. In *American Society for Engineering Education*. American Society for Engineering Education, 2012.

[10] V. Hayward and K. E. MacLean. Do it yourself haptics: part i. *Robotics & Automation Magazine, IEEE*, 14(4):88–104, 2007.

[11] M. Kilchenman and M. Goldfarb. Force saturation, system bandwidth, information transfer, and surface quality in haptic interfaces. In *Robotics and Automation, 2001. Proceedings 2001 ICRA. IEEE International Conference on*, volume 2, pages 1382–1387. IEEE, 2001.

[12] D. Kubus, I. Weidauer, and F. M. Wahl. 1khz is not enoughhow to achieve higher update rates with a bilateral teleoperation system based on commercial hardware. In *Intelligent Robots and Systems, 2009. IROS 2009. IEEE/RSJ International Conference on*, pages 5107–5114. IEEE, 2009.

[13] J. S. Mehling, J. E. Colgate, and M. A. Peshkin. Increasing the impedance range of a haptic display by adding electrical damping. In *Eurohaptics Conference, 2005 and Symposium on Haptic Interfaces for Virtual Environment and Teleoperator Systems, 2005. World Haptics 2005. First Joint*, pages 257–262. IEEE, 2005.

[14] M. K. OMalley, K. S. Sevcik, and E. Kopp. Improved haptic fidelity via reduced sampling period with an fpga-based real-time hardware platform. *J. Comput. Inf. Sci. Eng*, 9(1):1–7, 2009.

[15] R. Pintelon and J. Schoukens. *System Identification: A Frequency Domain Approach*, chapter 4: Design of Excitation Signals. Wiley, 2004.

[16] C. Richard, A. M. Okamura, and M. R. Cutkosky. Getting a feel for dynamics: Using haptic interface kits for teaching dynamics and controls. In *1997 ASME IMECE 6th Annual Symposium on Haptic Interfaces, Dallas, TX, Nov*, pages 15–21, 1997.

[17] C. E. Wong and A. M. Okamura. The snaptic paddle: a modular haptic device. In *Eurohaptics Conference, 2005 and Symposium on Haptic Interfaces for Virtual Environment and Teleoperator Systems, 2005. World Haptics 2005. First Joint*, pages 537–538. IEEE, 2005.